Table 1 Laminate configurations of $[(\theta_1)_{h_1}/(\theta_2)_{h_2}/(\theta_3)_{h_3}/(\theta_4)_{h_4}]_S$ corresponding to in-plane lamination parameters

$(\xi_1, \xi_2, \xi_3, \xi_4)$	θ_1, deg	θ_2, deg	θ_3, deg	θ_4, deg	h_1	h_2	h_3	h_4
(0.1, −0.2, 0.4, 0.6)	32.8	−64.3	10.8	77.0	0.51	0.22	0.15	0.12
(0.5, 0.5, 0, −0.2)	−9.2	64.0	9.2	−64.0	0.46	0.18	0.26	0.10
(0.3, 0.4, 0.4, 0)	22.2	−76.2	3.5	64.6	0.17	0.06	0.44	0.33

Table 1 shows examples of laminate configurations for some sets of $(\xi_1, \xi_2, \xi_3, \xi_4)$. The method for determining the laminate configurations corresponding to the out-of-plane lamination parameters $(\xi_9, \xi_{10}, \xi_{11}, \xi_{12})$ is similar. The layer angles are obtained using Eq. (9). The layer thicknesses of the $[(\theta_1)_{\bar{h}_1}/(\theta_2)_{\bar{h}_2}/(\theta_3)_{\bar{h}_3}/(\theta_4)_{\bar{h}_4}]_S$ laminate are determined from the following relations:

$$\bar{h}_j = \sqrt[3]{h_j + h_{j+1} + \cdots + h_4} - \sqrt[3]{h_{j+1} + \cdots + h_4}, \quad (j = 1, 2, 3, 4) \tag{12}$$

where h_j is the thickness component shown in Eq. (11).

Conclusions

The present paper has shown a stiffness design method of symmetric laminates using lamination parameters. The relation between the lamination parameters in symmetric laminates has been obtained. The method has been shown for determining the laminate configurations corresponding to the in-plane lamination parameters $(\xi_1, \xi_2, \xi_3, \xi_4)$ or out-of-plane lamination parameters $(\xi_9, \xi_{10}, \xi_{11}, \xi_{12})$. The limitation of the conventional laminates has also been discussed from the design viewpoint.

References

[1]Tsai, S. W., and Hahn, H. T., *Introduction to Composite Materials*, Technomic, Lancaster, PA, 1980.

[2]Fukunaga, H., and Vanderplaats, G. N., "Stiffness Optimization of Orthotropic Laminated Composites Using Lamination Parameters," *AIAA Journal*, Vol. 29, No. 4, 1991, pp. 641-646.

[3]Miki, M., and Fujii, T., "Material Design of Laminated Fibrous Composites with Required Bending-Twisting Coupling," *Materials System*, Vol. 4, June 1985, pp. 61-65 (in Japanese).

[4]Grenestedt, J. L., "Layup Optimization Against Buckling of Shear Panels," *Structural Optimization*, Vol. 3, July 1991, pp. 115-120.

Vibration of Compressively Loaded Shear Deformable Flat Panels Exhibiting Initial Geometric Imperfections

L. Librescu*
Virginia Polytechnic Institute and State University, Blacksburg, Virginia 24061
and
M. Y. Chang†
National Chung-Hsing University, Taichung, Taiwan 40227, Republic of China

Received Feb. 28, 1992; revision received April 3, 1992; accepted for publication April 20, 1992.

*Professor, Engineering Science and Mechanics Department.
†Associate Professor, Mechanical Engineering Department.

Introduction

ONE of the features characterizing the design of next-generation aeronautical/aerospace vehicles consists of the incorporation of advanced composite materials in their construction. For a more rational design of these structures as well as for a more exhaustive utilization of their unique properties, a better knowledge of their response characteristics is needed.

As is well known, composite material structures, in contrast to their metallic counterparts, exhibit high flexibilities in transverse shear, which, in many instances, result in detrimental effects. In the case of an orthotropic body, the transverse flexibilities are measured in terms of the ratios $E_\alpha/G_{\alpha 3}$ $(\alpha = 1, 2)$, whereas in the case of a transversely isotropic material, they are measured in terms of the ratio E/G', where $E_\alpha(E)$ and $G_{\alpha 3}(G')$ denote the in-plane Young's and transverse shear moduli, respectively. One of the goals of this Note is to assess the influence played by the transverse shear flexibility effect on small-amplitude vibrations of homogeneous/composite laminated panels compressed by edge loads in the pre- and postbuckling ranges. Because of the importance played by the unavoidable geometric imperfections and by the character of in-plane boundary conditions, their influence on the considered problem will also be investigated.

In spite of its evident importance, the study of the vibrational behavior of preloaded imperfect composite panels was done, with the exception of Ref. 1 within the classical Kirchhoff's model. It could easily be inferred, however, that employment of this model, postulating an infinite rigidity in transverse shear, instead of a more refined one incorporating this effect, will result, in many instances, in erroneous predictions of the response characteristics. In connection with the problem considered herein, the illustration of this statement will be given later in the paper.

Basic Assumptions: Governing Equations

The case of a flat plate of uniform thickness h symmetrically laminated of $2m + 1 (m = 1, 2, \ldots)$ transversely isotropic elastic layers is considered. It is assumed that the planes of isotropy of each material layer are parallel at each point to the reference plane of the composite panel (selected to coincide with the midplane of the midlayer).

It is assumed that the layers are in perfect bond, implying that no slip between two contiguous layers may occur.

The points of the three-dimensional space of the plate are referred to a set of rectangular Cartesian normal system of coordinates x_i, where x_α $(\alpha = 1, 2)$ denotes the in-plane coordinates, whereas x_3 denotes the normal one to the plane $x_3 = 0$ (defining the reference plane). Extension to the dynamic case of the geometrically nonlinear higher-order shear-deformable theory (HSDT) of laminated plates developed for the static case in Ref. 2 results in the following governing equations:

$$D\nabla^4 u_3 - c_{\alpha\omega}c_{\beta\rho}\{[u_{3,\alpha\beta} + \mathring{u}_{3,\alpha\beta}]F_{,\omega\rho} - \Omega\nabla^2[F_{,\omega\rho}(u_{3,\alpha\beta} + \mathring{u}_{3,\alpha\beta})]\}$$

$$+ m_0\left\{\ddot{u}_3 - \left(\frac{B+C}{S} + \delta_A\delta_B\left[\frac{R}{m_0} - \frac{M}{S}\right]\right)\nabla^2\ddot{u}_3\right\} = 0 \tag{1a}$$

$$(\tilde{b}+\tilde{c})\nabla^4 F + \tfrac{1}{2}[\nabla^2 u_3 \nabla^2 u_3 - u_{3,\lambda\rho}u_{3,\lambda\rho}]$$
$$+ [\nabla^2 \mathring{u}_3 \nabla^2 u_3 - \mathring{u}_{3,\pi\alpha}u_{3,\alpha\pi}] + 2\delta_A\tilde{d}[\nabla^2 u_{3,\rho}u_{3,\rho} + u_{3,\lambda\rho}u_{3,\lambda\rho}$$
$$+ \nabla^2 \mathring{u}_{3,\rho}u_{3,\rho} + \nabla^2 u_{3,\rho}\mathring{u}_{3,\rho} + 2\mathring{u}_{3,\rho\pi}u_{3,\pi\rho}] = 0 \qquad (1b)$$

$$\Gamma - \frac{C}{S}\nabla^2\Gamma = 0 \qquad (1c)$$

In Eqs. (1), $\Omega[\equiv (B+C)/S - \delta_A M/S]$ denotes a reduced stiffness parameter incorporating transverse shear effect; $F[\equiv F(x_\omega; t)]$ the Airy's potential function associated with the membrane stress resultants; u_3 $[\equiv u_3(x_\omega, t)$ and $\mathring{u}_3$ $(\equiv \mathring{u}_3(x_\omega)]$ the transverse displacement (measured from the imperfect surface) and the initial out-of-plane stress-free geometrical imperfection, respectively; D, A, B, C, R, M, S, $\tilde{b}$, $\tilde{c}$, $\tilde{d}$ the rigidity quantities defined in Ref. 2; m_0 the reduced mass; $c_{\alpha\beta}$ the two-dimensional permutation symbol; $\nabla^2(\equiv\Delta)$ the two-dimensional Laplace operator; $\Gamma[\equiv \Gamma(x_\omega; t)]$ the potential function associated with the boundary-layer effect[2,3]; δ_A and δ_B two tracers identifying the static and dynamic contributions of s_{33} (i.e., of the transverse normal component of Piola-Kirchhoff stress tensor) in the governing equations.

Einsteinian's summation convention is used in Eqs. (1) where the Greek indices range from 1 to 2, partial differentiation is denoted by a comma $(\cdot)_{,\alpha} \equiv \partial(\cdot)/\partial x_\alpha$ and $(\dot{\cdot}) \equiv \partial(\cdot)/\partial t$.

The dynamic governing system (1) incorporates the effects of transverse shear deformation and transverse normal stress, the geometric nonlinearities (in the Kármán's sense) as well as the dynamic and the initial geometric imperfection effects. Its specialization for the first-order transverse shear deformation (FSDT) and classical (CLT) theories can be accomplished by following Ref. 2.

Restricting our considerations to the case of rectangular $(l_1 \times l_2)$ panels simply supported on the whole contour and extending to the dynamic case the procedure outlined in Refs. 2 and 3, the following nonlinear equations governing the vibrational behavior of laminated composite flat panels compressed by the biaxial edge loads $\tilde{L}_1$ and $\tilde{L}_2$ is obtained:

$$-m_0[1+\Omega\pi^2/l_1^2(m^2+n^2\phi^2)]\ddot{f}_{mn} + [\tilde{L}_1\lambda_m^2 + \tilde{L}_2\mu_n^2](f_{mn}+\mathring{f}_{mn})$$
$$+\Omega[\tilde{L}_1\lambda_m^4 + \tilde{L}_2\mu_n^4](f_{mn}+\mathring{f}_{mn}) + \Omega(\tilde{L}_1+\tilde{L}_1)(f_{mn}+\mathring{f}_{mn})\mu_n^2\lambda_m^2$$
$$= D(\lambda_m^2+\mu_n^2)^2 f_{mn} + 2(f_{mn}^2 + 2f_{mn}\mathring{f}_{mn})(f_{mn}+\mathring{f}_{mn})\mu_n^2\lambda_m^2(\tilde{A}_1$$
$$+\tilde{A}_2) + 2\Omega(f_{mn}^2 + 2f_{mn}\mathring{f}_{mn})(f_{mn}+\mathring{f}_{mn})[\tilde{A}_1\lambda_m^2\mu_n^4 + \tilde{A}_2\lambda_m^4\mu_n^2$$
$$+\tilde{A}_1\lambda_m^4\mu_n^2 + \tilde{A}_2\lambda_m^2\mu_n^4], \quad (m,n) = (\overline{1,M}, \overline{1,N}) \quad \sum_{m,n} \qquad (2)$$

where the sign $\sum_{m,n}$ indicates the absence of summation over the indices m and n. Here, $\phi = l_1/l_2$; $f_{mn}[\equiv f_{mn}(t)]$, and $\mathring{f}_{mn}$ denote the amplitudes of transversal deflection and of initial geometric imperfections, respectively; $\lambda_m = m\pi/l_1$; $\mu_n = n\pi/l_2$; and $\tilde{A}_i (i = 1, 2, 3)$ are coefficients not displayed here. Equations (2) could accommodate also the case of the immovable edges $x_2 = 0, l_2$. The procedure yielding such a conversion was described in Refs. 2 and 3.

In order to determine the linear frequency-edge load interaction in both the pre- and postbuckling ranges, the case of small vibrations about the static previbration state is considered. In this case, the vibratory amplitude $f_{mn}(t)$ can be expressed as

$$f_{mn}(t) = \bar{f}_{mn} + \bar{\bar{f}}_{mn}(t) \qquad (3)$$

where $\bar{\bar{f}}_{mn}(t)$ is assumed small when compared to $\bar{f}_{mn}$ and $\mathring{f}_{mn}$ (in the sense of $\bar{\bar{f}}_{mn}^2 \ll \bar{f}_{mn}; \mathring{f}_{mn}$). Whereas the dependence of the static part $\bar{f}_{mn}$ of the amplitude upon the edge compressive loads may be determined from Eqs. (2) by discarding the inertia terms, the equation for the small-amplitude vibrations about the static configuration can be determined by substituting representation (3) into Eqs. (2) and omitting therein nonlinear terms of $\bar{\bar{f}}$.

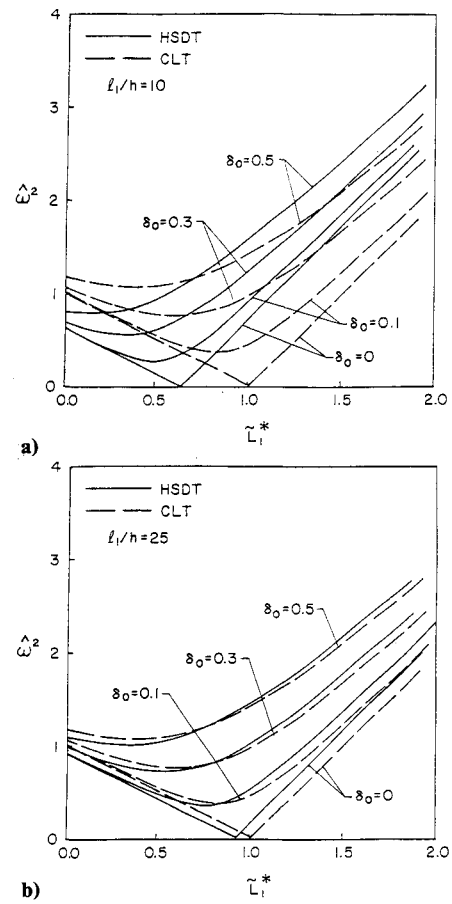

Fig. 1 Comparison of variation of fundamental frequency squared vs uniaxial compressive edge load for geometrically perfect and imperfect panels, $E/G' = 30$, $E/E' = 5$: a) moderately thick; b) moderately thin.

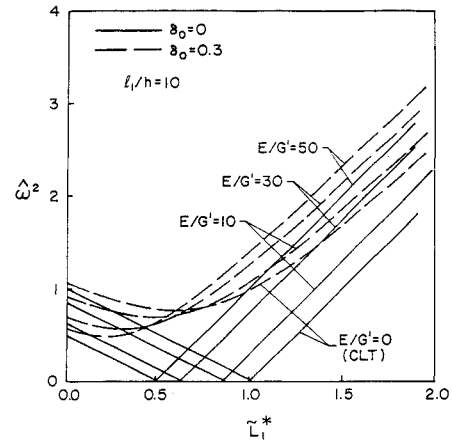

Fig. 2 Fundamental frequency squared vs uniaxial compressive edge loads for geometrically perfect and imperfect panels of moderate thickness exhibiting various flexibility ratios in transverse shear, $E/E' = 5$.

Further employment of $\bar{\bar{f}}_{mn} = \bar{f}\exp(i\omega_{mn}t)$, the equation describing the frequency-uniaxial/biaxial compressive edge load interaction is determined.

Results

The numerical illustrations concern the cases of single- and three-layered composite flat panels. For the latter, the cases labeled as case 1 and case 2, described in Ref. 2 are used here.

Within case 1, the face-layers exhibit, as compared to the core layer, a higher flexibility in transverse shear, whereas

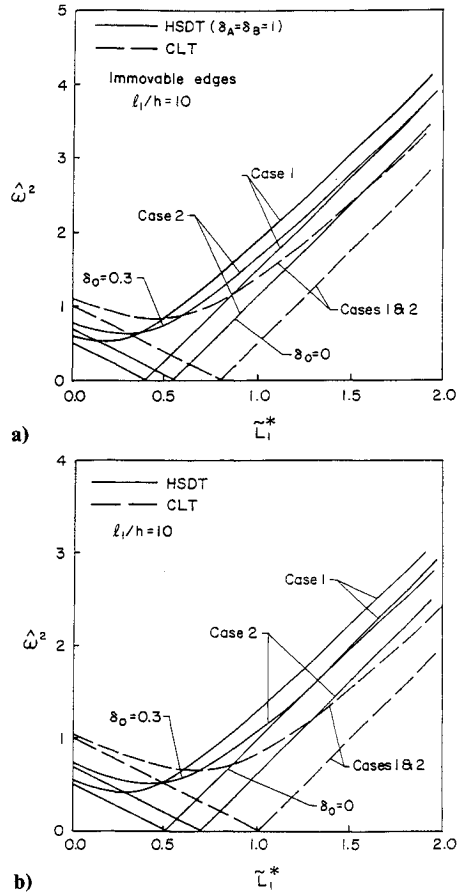

Fig. 3 Influence of in-plane edge conditions on fundamental frequency squared vs uniaxial compressive edge loads for geometrically perfect and imperfect panels of moderate thickness. The two cases of composite panels are considered: a) immovable edge conditions; b) movable edge conditions.

within case 2, the opposite feature takes place. Throughout the numerical examples, the case of square panels ($l_1 = l_2 \equiv l$) was considered.

Within the numerical illustrations, $\tilde{L}_1^* \equiv \tilde{L}_1/L_c$ denotes the reduced compressive load, where L_c denotes the buckling load in uniaxial compression predicted by the classical theory of its perfect plate counterpart, $\hat{\omega}^2 (\equiv \omega^2/\omega_c^2)$ denotes the ratio of the small-amplitude fundamental frequency squared of the actual shear deformable panel to its rigid in transverse shear counterpart obtained in unloaded conditions, while $\delta_o (\equiv \overset{o}{f}/h)$ denotes the nondimensional central initial deflection. The numerical results are condensed in Figs. 1–3, where the dependence of the reduced fundamental frequency squared $\hat{\omega}^2$ upon the reduced uniaxial load $\tilde{L}_1^*$ was diagrammatically represented.

Conclusions

The numerical results allow one to outline the conclusions:

1) In the prebuckling range (or for geometrically imperfect plates in the precritical one), the natural frequency predicted by the shear deformable plate theory is smaller than the one associated with its rigid in transverse shear counterpart. However, in the postbuckling/postcritical range, the opposite behavior takes place (see Figs. 1–3). Physically, this reverse in behavior is due to the fact that the shear deformable plates experience larger deflections than their rigid in transverse shear counterparts. As a result, larger tensile membrane stresses are generated in the postbuckling range, which in turn produce a stiffening of the plate. This reverts to the conclusion that the frequency predictions based on the classical plate theory are always inadvertently overestimated in the prebuckling range and underestimated in the postbuckling one.

2) With the increase of transverse shear flexibility, bigger differences between the frequencies predicted by shear deformable and infinitely rigid in transverse shear theories, both in the prebuckling/precritical and postbuckling/post-critical ranges are experienced (Fig. 2). In the case of composite panels, larger or lower differences as compared to the classical predictions are experienced, depending on whether the face layers are more transverse shear deformable than the core layer (case 1) or if the opposite case (case 2) takes place, respectively (see Figs. 3). This conclusion remains valid for both the perfect and geometrically imperfect plates as well. As the plate becomes thinner, the differences tend to decay (see Figs. 1a and 1b).

3) The results displayed in Figs. 1 and 3 reveal that in the precritical range, the vibration frequency predicted by both the classical and shear deformable theories of single- or multilayered plates may be significantly raised by the geometric imperfections. This is in sharp contrast to the behavior of perfect plates (single- or multi-layered ones) where the squared natural frequency decreases linearly in the prebuckling range with increasing compressive in-plane loading.

4) The character of in-plane boundary conditions (i.e., immovable or movable ones) plays a great role not only in the decrease or increase of buckling loads but also in the increase or decrease of the vibratory frequencies. The results (see Figs. 3) reveal that, in the prebuckling range for geometrically perfect plates, the eigenfrequencies associated with free movable edges are higher than the ones associated with their immovable counterparts. However, for geometrically imperfect plates, the frequencies associated with immovable edge panels are higher over the entire range of compressive loads than their counterparts resulting in the case of free movable edges.

5) The FSDT provides reliable results, very close in fact, to the ones predicted by the HSDT. Here, like in the case of the static postbuckling, $K^2 = 5/6$ proves to be an excellent shear correction factor for single-layered plates, whereas $K^2 = 2/3$ turns out to be a better one in the case of multilayered plates.

6) A final comment concerns the fact that in the system of parameters $(\hat{\omega}^2, \tilde{L}_1^*)$ the classical plate theory provides results that are indifferent to the degree of transverse shear flexibility and thickness ratio (Figs. 1–3).

Although the analysis was restricted to the fundamental eigenfrequency, there are all the reasons to anticipate that the same trend will be followed, in general, by the other frequencies, as well. It is believed that the present conclusions, part of them, to the best of the authors' knowledge, formulated for the first time in the literature, will be useful toward a better understanding of the problem involving frequency-compressive load interaction of shear deformable laminated panels exhibiting initial geometric imperfections and different in-plane edge conditions.

Acknowledgment

The partial support of this work by NASA Langley Research Center through Grant NAG-1-1300 is gratefully acknowledged by the first author.

References

[1]Bhimarradi, A., "Non-Linear Free Vibration Analysis of Composite Plates with Initial Imperfections and In-Plane Loadings," *International Journal of Solids Structures,* Vol. 25, No. 1, 1989, pp. 33–43.

[2]Librescu, L., and Stein, M., "A Geometrically Nonlinear Theory of Transversely-Isotropic Laminated Composite Plates and Its Use in the Postbuckling Analysis," *Thin Walled Structures,* special issue of *Aeronautical Structures,* Vol. 11, Nos. 1 & 2, 1991, pp. 177–201.

[3]Librescu, L., and Stein, M., "Postbuckling Analysis of Shear Deformable Composite Flat Panels Taking Into Account Geometrical Imperfections," *Proceedings of the AIAA/ASME/ASCE/AHS/ASC 31st Structures, Structural Dynamics and Materials Conference,* CP902, Pt. 2, AIAA, Washington, DC, 1990, pp. 892–902 (AIAA Paper 90-0967). (Amended version, *AIAA Journal,* Vol. 30, No. 5, 1992, pp. 1352–1360.)